




RESEARCH ARTICLE

Hederasaponin C inhibits LPS-induced acute kidney injury in mice by targeting TLR4 and regulating the PIP2/NF- κ B/NLRP3 signaling pathway

Shan Han^{1,2} | Siyuan Li² | Jilang Li³ | Jia He^{1,2} | Qin-Qin Wang^{1,2} |
Xiang Gao² | Shilin Yang² | Jingjing Li⁴  | Renyikun Yuan²  |
Guoyue Zhong^{1,3} | Hongwei Gao² 

¹Research Center for Traditional Chinese Medicine Resources and Ethnic Medicine, Jiangxi University of Chinese Medicine, Nanchang, China

²College of Pharmacy, Guangxi University of Chinese Medicine, Nanning, China

³National Pharmaceutical Engineering Center for Solid Preparation in Chinese Herbal Medicine, Jiangxi University of Chinese Medicine, Nanchang, China

⁴Department of Rehabilitation Sciences, Faculty of Health and Social Sciences, Hong Kong Polytechnic University, Hong Kong, China

Correspondence

Renyikun Yuan and Hongwei Gao, College of Pharmacy, Guangxi University of Chinese Medicine, Nanning 530000, China.

Email: yryk0808@163.com and gaohongwei06@126.com

Guoyue Zhong, Research Center for Traditional Chinese Medicine Resources and Ethnic Medicine, Jiangxi University of Chinese Medicine, Nanchang 330004, China.
Email: zgy1037@163.com

Funding information

Guangxi Science and Technology Base and Talent Project, Grant/Award Number: 2022AC18022; China-ASEAN International Innovative Center for Health Industry of TCM, Grant/Award Number: AD20297142; Qihuang High-level Talent Team Cultivation Project of Guangxi University of Chinese Medicine, Grant/Award Number: 2021002; Innovation Project of Guangxi Graduate Education, Grant/Award Number: YCSW2019176; Guangxi University of Chinese Medicine, Grant/Award Number: 2022BS008; Guangxi University Young and Middle-Aged Teachers Research Basic Ability Improvement Project, Grant/Award Number: 2023KY0303; Jiangxi Province 2022 Annual Graduate Student

Abstract

Acute kidney injury (AKI) is a common clinical condition associated with increased incidence and mortality rates. Hederasaponin C (HSC) is one of the main active components of *Pulsatilla chinensis* (Bunge) Regel. HSC possesses various pharmacological activities, including anti-inflammatory activity. However, the protective effect of HSC against lipopolysaccharide (LPS)-induced AKI in mice remains unclear. Therefore, we investigated the protective effect of HSC against LPS-induced renal inflammation and the underlying molecular mechanisms. Herein, using MTT and LDH assays to assess both cell viability and LDH activity; using dual staining techniques to identify different cell death patterns; conducting immunoblotting, QRT-PCR, and immunofluorescence analyses to evaluate levels of protein and mRNA expression; employing immunoblotting, molecular docking, SPR experiments, and CETSA to investigate the interaction between HSC and TLR4; and studying the anti-inflammatory effects of HSC in the LPS-induced AKI. The results indicate that HSC inhibits the expression of TLR4 and the activation of NF- κ B and PIP2 signaling pathways, while simultaneously suppressing the activation of the NLRP3 inflammasome. In animal models, HSC ameliorated LPS-induced AKI and diminished inflammatory response and the level of renal injury markers. These findings suggest that HSC has potential as a therapeutic agent to mitigate sepsis-related AKI.

Abbreviations: AKI, acute kidney injury; ASC, apoptosis-associated speck-like protein containing a CARD; CETSA, cellular thermal shift assay; ELISA, enzyme-linked immunosorbent assay; HE, hematoxylin and eosin; IL-1 β , interleukin-1 β ; IL-6, interleukin-6; LPS, lipopolysaccharide; Lym, lymphocyte; NF- κ B, nuclear factor kappa-light-chain-enhancer of activated B cells; NEU, neutrophil; NLRP3, nucleotide-binding domain leucine-rich repeat and pyrin domain containing receptor 3; PIP2, phosphatidylinositol 4,5-bisphosphate; PLC, phospholipase C; SRP, surface plasmon resonance; TLR4, toll-like receptor 4; TNF- α , tumor necrosis factor- α ; WBC, white blood cell.

This is an open access article under the terms of the [Creative Commons Attribution-NonCommercial-NoDerivs](https://creativecommons.org/licenses/by-nc-nd/4.0/) License, which permits use and distribution in any medium, provided the original work is properly cited, the use is non-commercial and no modifications or adaptations are made.

© 2023 The Authors. *Phytotherapy Research* published by John Wiley & Sons Ltd.

Innovation Special Fund Project, Grant/Award Number: YC2022-B189

KEYWORDS

acute kidney injury, Hederasaponin C, lipopolysaccharide, PIP2/NF- κ B/NLRP3, TLR4

1 | INTRODUCTION

Acute kidney injury (AKI) is a major health problem characterized by acute loss of kidney function, which affects 13.3 million people each year and is characterized by increased and high mortality (Vázquez-Carballo et al., 2021). Sepsis is an acute systemic inflammatory response syndrome caused by infectious agents; the kidney is one of the major target organs and 29.8% of septic patients developed AKI (Oweis et al., 2020). Therefore, it is urgent to develop a drug for improving and preventing kidney injury.

Toll-like receptor 4 (TLR4) have been identified as key regulators of inflammatory processes, significantly contributing to the pathogenesis of AKI (Vallés et al., 2023). Kidney injury elicits TLR4 activation, triggering the activation of downstream signal transduction pathways, including NLRP3 inflammasome assembly (Vallés et al., 2023). Prior research indicated that TLR4 inhibition could diminish kidney damage and reduce inflammatory cytokine production (Li, Zou, et al., 2021). The activation of the NLRP3 inflammasome promotes pro-caspase-1 and pro-IL-1 β maturation. Studies reported that inhibition of NLRP3 inflammasome activation lessens kidney injury. Contemporary research underscores the vital role of the NLRP3 inflammasome, a cytoplasmic macromolecular complex, in kidney inflammation modulation, the PIP2 hydrolysis by PLC γ 2 generates IP3 and DAG, which subsequently influences Ca²⁺ and activates the NLRP3 inflammasome (Yuan et al., 2022). The binding of LPS to TLR4 prompts the activation of the transcription factor nuclear factor-kappa B (NF- κ B). Once activated, NF- κ B migrates into the nucleus, where it modulates immune responses and inflammation responses by releasing inflammatory mediators, such as TNF- α and IL-6 (Han et al., 2019). Studies have found that protein kinase PKC can also regulate the phosphorylation of P65 (Lozano et al., 1994). Thu-HuyenPham and others have also proven that PKC is an upstream regulator of NF- κ B (Pham et al., 2017). It was discovered by J. Wu et al. that by inhibiting the phosphorylation of TAK1, the activation of downstream signal cascades and thus the activation of NF- κ B can be further suppressed (Wu et al., 2013). Thus, the TLR4/NLRP3 pathway plays a crucial role in the AKI process.

HSC is a compound derived from *Pulsatilla chinensis* (Bunge) Regel, with a long history of utilization in Chinese medicine due to its fever-reducing, detoxifying, anti-dysenteric, and dampness-drying properties (He et al., 2020; Jin et al., 2018). HSC possesses significant antioxidant (Gülçin et al., 2004), anti-inflammatory activity (Gepdiremen et al., 2005), relieves acute lung injury (Han et al., 2022), and alleviates acute colitis (Zhou et al., 2022). Nevertheless, the therapeutic efficacy of HSC and its mode of action in AKI still lack clarity. This study utilized the LPS-induced AKI model and LPS + ATP-

induced HK2 cells to investigate the inflammation-regulating mechanisms of HSC in AKI.

2 | METHODS

2.1 | Reagents and chemicals

Hederasaponin C (HSC) (>98%) was isolated from the *Pulsatilla chinensis* (Bunge) Regel in our laboratory and determined by HPLC. LPS (Lipopolysaccharides from *Escherichia coli* O111:B4, S1732) was purchased from Beyotime (Shanghai, China). Antibodies against p65 (#8242 T), p-p65 (#3033), PKC α (#2056S), p-PKC α (#9375S), TAK1 (#4505), p-TAK1 (#9339), Cleaved-IL-1 β (#63124), NLRP3 (#15101), IL-1 β (#31202), Cleaved-Caspase-1 (#89332), ASC (#13833), PLC γ 2 (#3872), DAG Lipa α (#13626), IP3 Receptor1 (#8568), and GAPDH (#5174) were purchased from Cell Signaling Technology (Beverly, MA, USA). Caspase-1 (ab1872) were purchased from Abcam (Cambridge, MA, USA). PIP2 (#53412) were purchased from Senta (Santa Cruz Biotechnology, USA). TNF- α (#234889-001), IL-6 (#225266-022), and IL-1 β (#224603-014) ELISA kits were purchased from Invitrogen (Vienna, Austria).

2.2 | Cell culture and treatment

The HK-2 cell line was obtained from Pricella (Procell Life Science & Technology Co., Ltd.) and cultured in DMEM/F-12 medium supplemented with 10% FBS and 1% penicillin-streptomycin. The septic model was established in vitro by incubating the HK-2 cells with 1 μ g/mL LPS (Liu et al., 2023) for 6 h followed by incubation with 10 mM ATP for 2 h.

2.3 | Cell viability assay

The viability of LPS + ATP-induced HK-2 cells in each group was measured using MTT assay following the manufacturer's instructions. We incubated HK-2 cells at concentrations of HSC (0, 10, 20, and 40 μ M) (Han et al., 2022) for 24 h to determine the cytotoxicity of HSC by assessing its cell viability. The cells were pre-treated with HSC (0, 10, 20, 40 μ M) for 4 h, and then treated with or without LPS and ATP. MTT solution (5 mg/mL) was added to each well and incubated for another 3 h at 37°C in the dark. The supernatant was removed, and then the cells were dissolved with DMSO (100 μ L/well). The absorbance was detected by a microplate reader at 570 nm.

2.4 | LDH release assay

The cells were pretreated with different concentrations of HSC (0, 10, 20, and 40 μ M) for 4 h, followed by treatment with or without LPS and ATP. Subsequently, the supernatants were collected and analyzed for lactate dehydrogenase (LDH) activity using the LDH Assay Kit (Beyotime Biotechnology, Shanghai, China) in accordance with the manufacturer's instructions. Finally, the absorbance values were measured at 450 nm using a multimode plate reader.

2.5 | Cell death detection with flow cytometry

Cellular apoptosis was assessed using the Annexin V-7AAD assay for detecting programmed cell death. HK-2 cells were seeded in 6-well plates and allowed to grow overnight. After a 4 h incubation with HSC, the cells were either treated with or without LPS and ATP. Subsequently, the cells were collected, washed with cold PBS, and resuspended in a $1 \times$ binding buffer. Following a 15-min staining at room temperature in the dark with Annexin V (5 μ M) and 7AAD (5 μ M), the samples were analyzed by flow cytometry (Becton-Dickinson, Bedford, MA, USA) and the acquired data were processed with the Flow Jo software (TreeStar, Ashland, OR, USA).

2.6 | Analysis of intracellular Ca^{2+} levels

The cells were exposed to 1 μ M Fluo-3/AM diacetate and incubated for 1 h at room temperature, while protected from light. Next, the cells were rinsed with PBS three times, and then observed under a fluorescence microscope (Green fluorescent marker for intracellular Ca^{2+} levels). Alternatively, the cells were harvested and assessed for Ca^{2+} levels using flow cytometry (Becton-Dickinson, Franklin Lakes, NJ, USA).

2.7 | Immunofluorescence assay

The cells were washed three times with PBS and subsequently fixed at room temperature for 30 min using 4% PFA. After fixation, the cells

were permeabilized for 15 min using 0.5% Triton X-100, and then blocked for 30 min with 5% BSA. Primary antibodies against NF- κ B/p65, PIP2, PLC γ 2, and Caspase-1 were incubated with the cell samples overnight at 4°C. The following day, the cells were incubated for 2 h at room temperature with Goat anti-mouse IgG Fluor® 488 Conjugate and Goat anti-Rabbit IgG Fluor® 594 Conjugate (red fluorescent label NF- κ B/P65, PLC γ 2, green fluorescent label PIP2 and Caspase-1). Finally, the cells were stained with Hoechst 33342 for 10 min and analyzed using a confocal laser scanning microscope (Leica TCS SP8, Solms, Germany).

2.8 | Quantitative real-time PCR (qRT-PCR) assay

After extracting the total RNA, 1 μ g of the RNA was subjected to qRT-PCR analysis using SYBR green dye. Oligonucleotide primers for TLR4, TAK1, PKC α , P65, TNF- α , IL-6, IL-1 β , NLRP3, Casp1, IL-1 β , and GAPDH were utilized during the PCR amplification process (Table 1).

2.9 | Western blotting analysis

Protein concentrations were determined using a BCA protein kit. The denatured proteins were separated with 8%, 10%, or 12% SDS-PAGE gels and transferred to PVDF membranes (Millipore, Billerica, MA, USA). After blocking PVDF membranes with 5% skim milk for 2 h, the PVDF membrane was incubated with primary antibodies (1:1000) overnight at 4°C. After washing with TBST, the membrane was incubated with a secondary antibody (1:5000) for 2 h at room temperature. The protein band signal was detected with SuperSignal West Femto maximum sensitivity substrate (Pierce Biotechnology) under visualization in a ChemiDoc MP Imaging System (Bio-Rad, Hercules, CA, USA). GAPDH was used as a housekeeping protein.

2.10 | Cellular thermal shift assay (CETSA)

The HEK293T cells underwent lysis with RIPA Lysis Buffer, consisting of 1% PMSF and 1% cocktail. Subsequently, the respective cell lysates

TABLE 1 Primer sequences.

Target	Forward primer	Reverse primer
TLR4	TGCCTTCACTACAGAGACT	ACACCACAACAATCACCTT
TAK1	CCGGTGAGATGATCGAAGCC	GCCGAAGCTCTACAATAAACGC
PKC α	GTCCACAAGAGGTGCCATGAA	AAGGTGGGGCTTCCGTAAGT
P65	ATGTGGAGATCATTGAGCAGC	CCTGGTCTGTGTAGCCATT
TNF- α	GAGGCCAAGCCCTGGTATG	CGGGCCGATTGATCTCAGC
IL-6	ACTCACCTCTTCAGAACGAATTG	CCATCTTTGGAAGTTTCAGGTTG
IL-1 β	ATGATGGCTTATTACAGTGGCAA	GTCGGAGATTCGTAGCTGGA
NLRP3	AGCCTCAACAAACGCTACAC	CATCTTAATGGGACTCACGG
Casp1	CAGACAAGGGTGCTGAACAA	TTCGGAATAACGGAGTCAAT
GAPDH	CAGGAGGCATTGCTGATGAT	GAAGGCTGGGGCTCATTT

were incubated alongside vehicle control (DMSO) or HSC (40 μ M) for 30 min while situated on ice. The mixture was then centrifuged at 14000 g for 30 min at 4°C. The supernatant was divided into six equal parts and heated at different temperatures (36, 40, 44, 48, 52, and 56°C) for 3 min. The solution was then cooled for 30 s at room temperature and analyzed using a western blotting assay.

2.11 | Molecular docking

We used Discovery Studio 4.5 and UCSF Chimera 1.7 to perform a molecular docking model of HSC with the 3D structure of TLR4 (PDB code: 3FXI). The regularized protein was analyzed to determine the important amino acids in the predicted binding pocket. Next, we performed interactive docking of all HSC conformers to the selected active site using LibDock, after energy minimization using the “prepares ligand” protocol. Finally, we assigned a score to the docked compound based on its binding mode onto the binding site.

2.12 | Surface plasmon resonance (SPR) analysis

SPR analysis was performed on a Biacore X100 (Cytiva, United States) instrument with CM5 sensor chip. Recombinant human TLR4 was immobilized in parallel-flow channels of CM5 chip by using amine-coupling kit. HSC was dissolved in HBS-EP buffer (Cytiva, United States), and series concentrations of HSC were injected into the flow system at the flow rate of 20 mL/min. The association time was 120 s and the dissociation time was 300 s. Binding kinetics were analyzed using Biacore X100 Control Software 2.0.2.

2.13 | HSC-biotin pulldown assay

HSC-biotin (40 μ M) was incubated with streptavidin agarose beads in a buffer solution (PBS at pH 7.4 with 0.05% Tween-20) at room temperature for a duration of 2 h. Following this, 10 μ L of streptavidin agarose beads, with HSC-biotin immobilized on them, was incubated further with His-TLR4 protein, at varying concentrations of HSC, and with 293 T-cell lysates expressing Flag-TLR4 in its wild type (WT) for another 2 h. After this incubation period, the beads were washed with the buffer solution and the bound proteins were subjected to Immunoblot (IB) analysis using Flag or His antibodies.

2.14 | Animals

Healthy male BALB/c mice (6–8 weeks old and 18–22 g weight) were obtained from the Hunan SJA Laboratory Animal Co., Ltd. (Hunan, China). All mice were housed under specific pathogen-free (SPF) conditions. All animal care and experimental procedures were under the approval of the Ethics Committee on Laboratory Animal Management

of Guangxi University of Chinese Medicine (Approval Document No. SYXK-GUI-2019-0001).

2.14.1 | LPS-induced AKI of mice

All mice were randomly divided into six groups ($n = 12$ per group): blank group, mold group (LPS, 2 mg/kg, i.p.) (Cui et al., 2021), HSC intraperitoneal injection (10, 20 and 40 mg/kg) and positive group (dexamethasone, DEX, 5 mg/kg, i.p.). Mice in all groups except the blank group were injected intraperitoneally with LPS (2 mg/kg, i.p.). After LPS treatment, the mice were administrated with HSC at 0 and 12 h. The positive group was administrated with DEX at 0 h after LPS treatment, and all experimental mice were dislocated and sacrificed after 24 h of LPS treatment. Blood samples were collected for measurement of neutrophil (NEU), white blood cell (WBC) and Lymphocyte (Lym), by using an auto hematology analyzer (Mindray, Shenzhen, China). The pro-inflammatory cytokines levels were detected by ELISA. The kidney tissue samples were detected by histological analysis. Fractions of kidney tissue samples were employed for immunoblotting. The remaining kidney tissue was employed for the detection of inflammatory cytokines.

2.14.2 | Kidney index

The kidney was obtained and weighed, and the kidney index of the mice was calculated as:

$$\text{kidney index (\%)} = \text{kidney weight (g)} / \text{body weight (g)} \times 100.$$

2.14.3 | Renal histopathology analysis

HE staining was used to observe the histological lesions. The kidney tissue was fixed in 4% paraformaldehyde for 24 h and replaced once with 4% paraformaldehyde solution, and then different concentrations of ethanol in turn for dehydration, decalcification, and paraffin embedding after sectioning, and then the sections were stained with hematoxylin–eosin. The pathological changes of the tissue were observed by optical microscope (UOP, DSZ5000X, China).

2.14.4 | Enzyme-linked immunosorbent assay (ELISA)

Centrifuge the blood for 15 min at 1000 g, 4°C and aspirate the supernatant as the serum sample. Kidney tissue was homogenized using a tissue grinder (TP-24, Jieliang instrument manufacturing Tianjin Co., Ltd, Tianjin, China) and then the supernatant was collected after centrifugation at 3000 rpm, 4°C for 15 min and placed at -80°C . Pro-inflammatory cytokines such as TNF- α , IL-1 β and IL-6 were measured in all samples using ELISA kits according to the manufacturer's instructions.

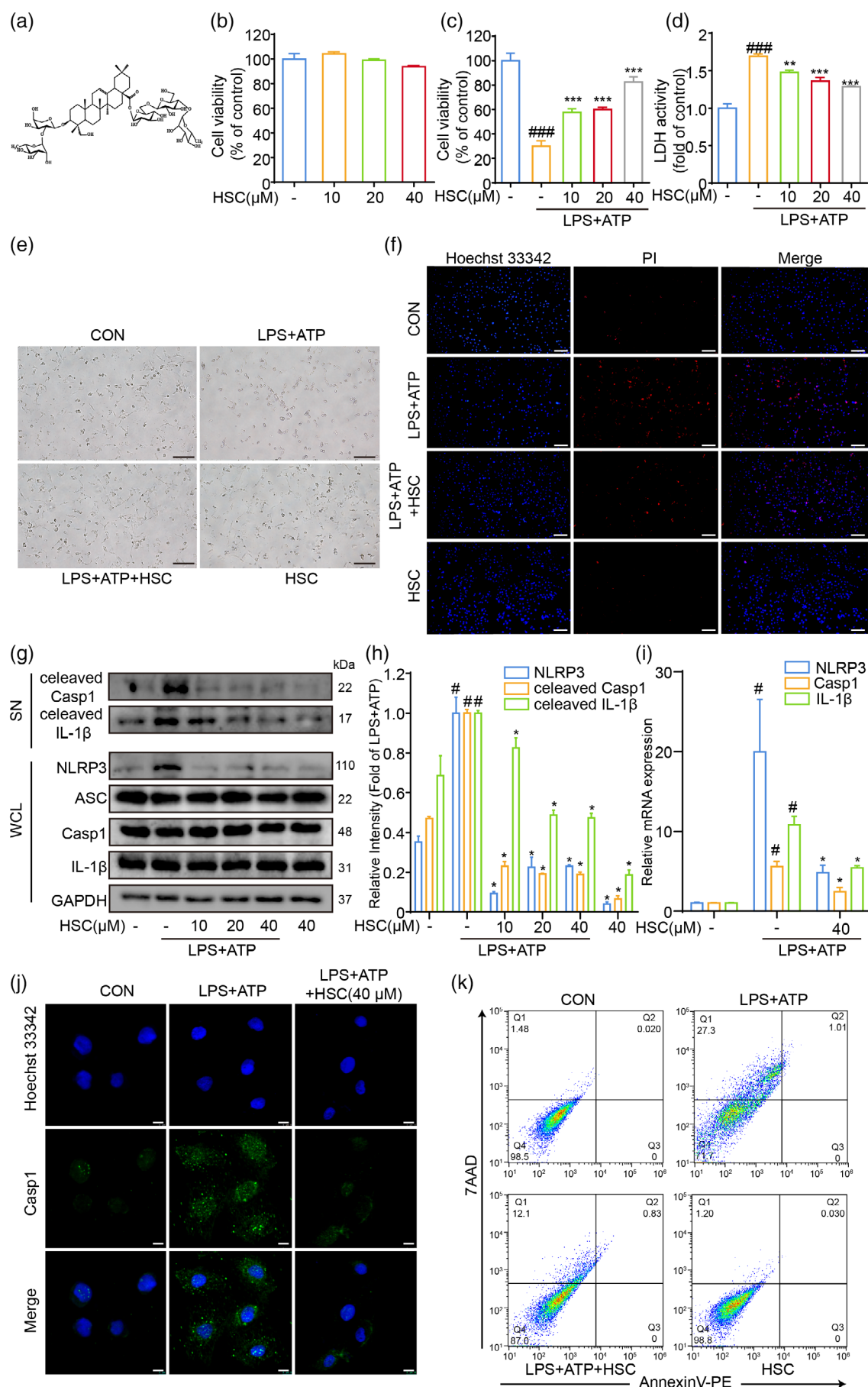


FIGURE 1 Legend on next page.

2.15 | Statistical analysis

All experiments were repeated as the mean \pm SD from at least three times. Analysis of statistical significance was performed using GraphPad Prism 6.0 software (GraphPad Software, San Diego, CA). One-way ANOVA and Dunnett's multiple comparison test were used for comparison between groups. A p -value of < 0.05 indicated a significant difference.

3 | RESULTS

3.1 | HSC suppresses NLRP3 inflammasome activation in LPS + ATP-induced HK2 cells

The cytotoxic effect of HSC on HK-2 cells was detected by MTT (Figure 1a). Figure 1b shows that HSC almost has no cytotoxicity at concentrations of 10, 20, or 40 μ M, maintaining a cell viability rate of over 95%. HSC effectively prevented cell death induced by LPS + ATP in HK-2 cells, as confirmed by MTT and LDH assays (Figure 1c–e). PI staining confirmed that LPS + ATP-induced cell death in HK-2 cells was necrotic, demonstrated by increased PI fluorescence, which was mitigated by HSC (40 μ M) treatment (Figure 1f). Figure 1k demonstrates that the dual staining with Annexin V and 7-AAD revealed the LPS + ATP-induced cell death (Annexin V⁺, 7-AAD⁺). Pre-treatment with HSC effectively reverses cell death in HK-2 cells. The possible activation of the NLRP3 inflammasome in tubular epithelial cells in LPS + ATP-induced HK2 cells was explored by examining the markers of inflammasome including NLRP3, ASC, post-translational processing of caspase-1 (cleaved caspase-1, Caspase-1 P20), and cleaved IL-1 β . Figure 1g,h shows that stimulation of HK-2 cells with LPS + ATP led to a significant increase in NLRP3, cleaved caspase-1, and cleaved IL-1 β protein expression, which was notably reduced by pre-treatment with HSC. Furthermore, HSC significantly reduced the mRNA levels of NLRP3, caspase-1, and IL-1 β in LPS + ATP-stimulated HK-2 cells (Figure 1i). HSC also attenuated the activation of caspase-1 in LPS + ATP-treated HK-2 cells (Figure 1j). These findings suggest that stimulation with LPS + ATP triggers activation of the NLRP3 inflammasome in HK-2 cells, which can be effectively suppressed by HSC treatment.

3.2 | HSC inhibited the activation of PIP2 signaling pathway in LPS + ATP-induced HK-2 cells

Central to the inflammatory cascade, calcium ions (Ca^{2+}) have been demonstrated to destabilize mitochondria upon increased intracellular concentration. This event subsequently activates the NLRP3 inflammasome, accelerating inflammatory responses (Wang et al., 2020). The enzyme PLC γ 2 is recognized for hydrolyzing PIP2 into IP3 and DAG. This action triggers the discharge of calcium ions from internal storage or stimulates PKC to control subsequent signaling processes (Suh et al., 2008). Figure 2a–c elucidates the implications, where Western blotting assays illustrate an upregulated expression of PIP2, DAG, and IP3 proteins and a downregulated PLC γ 2 in LPS + ATP-stimulated HK-2 cells. Nevertheless, the HSC pretreatment resulted in a significant decrease in PIP2, IP3, and DAG protein expressions, while concurrently upregulating PLC γ 2 expression. This was confirmed via immunofluorescence assays showing a marked increase in PIP2 fluorescence (green) in LPS-induced HK-2 cells, an increase significantly reduced by HSC intervention (Figure 2g). Therefore, HSC appears to be an effective inhibitor of PIP2 expression. With LPS + ATP stimulation, PLC γ 2 fluorescence (red) was decreased but was markedly enhanced with HSC treatment, suggesting an HSC-induced increase in PLC γ 2 expression (Figure 2h). Within this context, the PIP2 pathway, situated on the membrane, controls the release of Ca^{2+} from the endoplasmic reticulum. Further validating this, fluorescence microscopy and flow cytometry assays (Figure 2d–f) showed a significant surge in Ca^{2+} levels after LPS + ATP treatment. Nevertheless, HSC was found to effectively block this Ca^{2+} release, leading to the reduction of intracellular Ca^{2+} concentration. These observations suggest that LPS + ATP stimulation activates the PIP2 pathway in HK-2 cells, an activation effectively inhibited by HSC treatment.

3.3 | HSC inhibited the NF- κ B signaling pathway in LPS + ATP-induced HK-2 cells

NF- κ B activation is regulated by various kinase signaling pathways and other factors (Wu et al., 2017). TAK1 is a key kinase in TLR4-mediated NF- κ B activation. Prior research highlighted the role of Ro 31-8220, a PKC inhibitor, in suppressing LPS-activated P65 nuclear translocation in J774A.1 cells (Banerjee et al., 2020). As

FIGURE 1 HSC suppresses NLRP3 inflammasome activation in LPS + ATP-induced HK2 cells (a) Showcases the chemical structure of HSC. (b) The MTT assay confirmed the viability of HK-2 cells after 24 h treatment with HSC. (c, d) The cell viability and LDH activity were measured. (e) HSC (40 μ M) inhibited the morphological changes in HK-2 cells mediated by LPS + ATP (Scale bar = 100 μ m). (f) The progression of PI uptake in HK-2 cells was observed under a fluorescence microscope (Scale bar = 100 μ m). (g) Western blotting was used to detect the expressions of NLRP3, ASC, pro-caspase-1 (CASP1), cleaved-CASP1, pro-IL-1 β , and cleaved-IL-1 β proteins in HK-2 cells. (h) A statistical comparison was conducted on the content of NLRP3, cleaved-CASP1, and cleaved-IL-1 β across different groups. (i) RT-qPCR assay was used to quantify the mRNA levels of NLRP3, CASP1, and IL-1 β in HK-2 cells. (j) CASP1 activation was assessed through immunofluorescence (scale bar = 10 μ m). (k) The occurrence of LPS + ATP-induced pyroptosis in HK-2 cells was confirmed through an Annexin V and 7-AAD double staining assay. Results are shown as mean \pm SD. # $p < 0.05$, and ### $p < 0.001$ vs. control group. * $p < 0.05$, ** $p < 0.01$, and *** $p < 0.001$ vs. LPS + ATP group, $n = 3$.

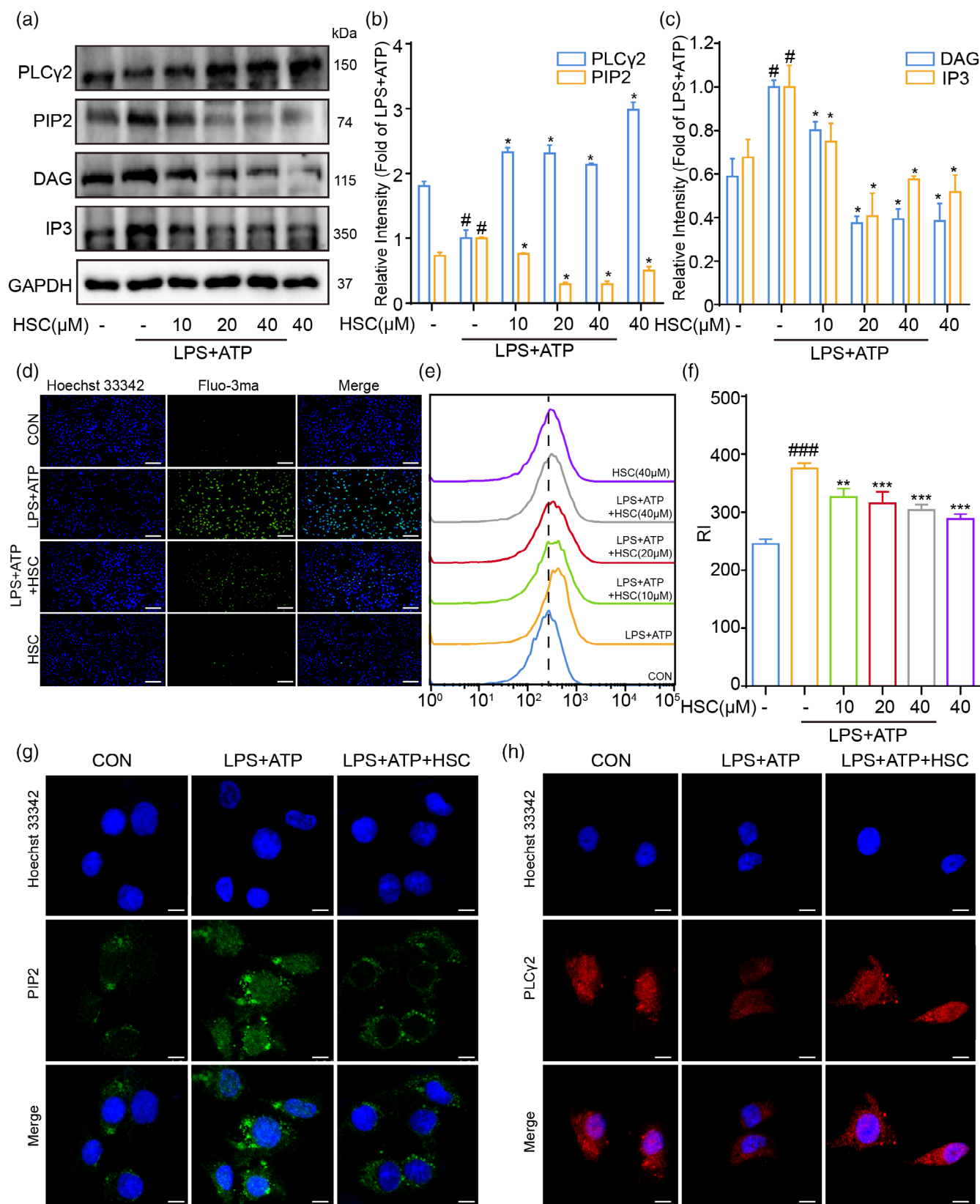


FIGURE 2 HSC inhibited the activation of PIP2 signaling pathway in LPS + ATP-induced HK-2 cells (a) Expression levels of PLCγ2, PIP2, DAG, and IP3 were assessed via immunoblotting. (b, c) statistical analysis was performed to compare the quantities of PLCγ2, PIP2, DAG, and IP3 in different groups. (d) Cells were stained with Fluo-3 AM, a Ca²⁺ indicator, and the resulting fluorescence intensity was measured using a fluorescence microscope (scale bar = 100 μm). (e, f) Ca²⁺ levels were investigated by staining cells with Fluo-3 AM and analyzing the results using flow cytometry. (g, h) The expression levels of PIP2 and PLCγ2 were evaluated using fluorescence microscope (scale bar = 10 μm). #p < 0.05 and ###p < 0.001 indicate a significant difference relative to the control group, while *p < 0.05, **p < 0.01, and ***p < 0.001 highlight a significant difference relative to the LPS + ATP group, n = 3.

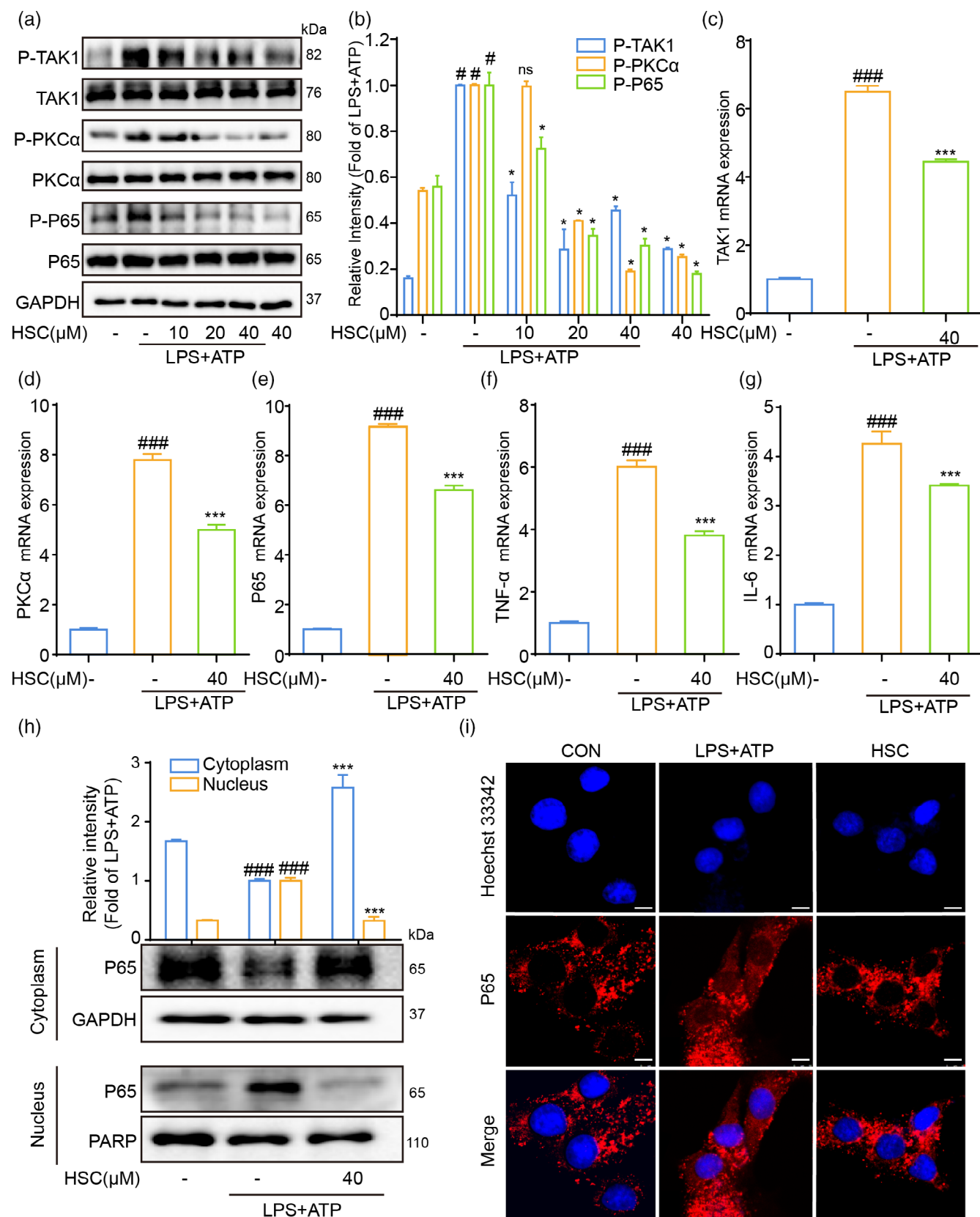
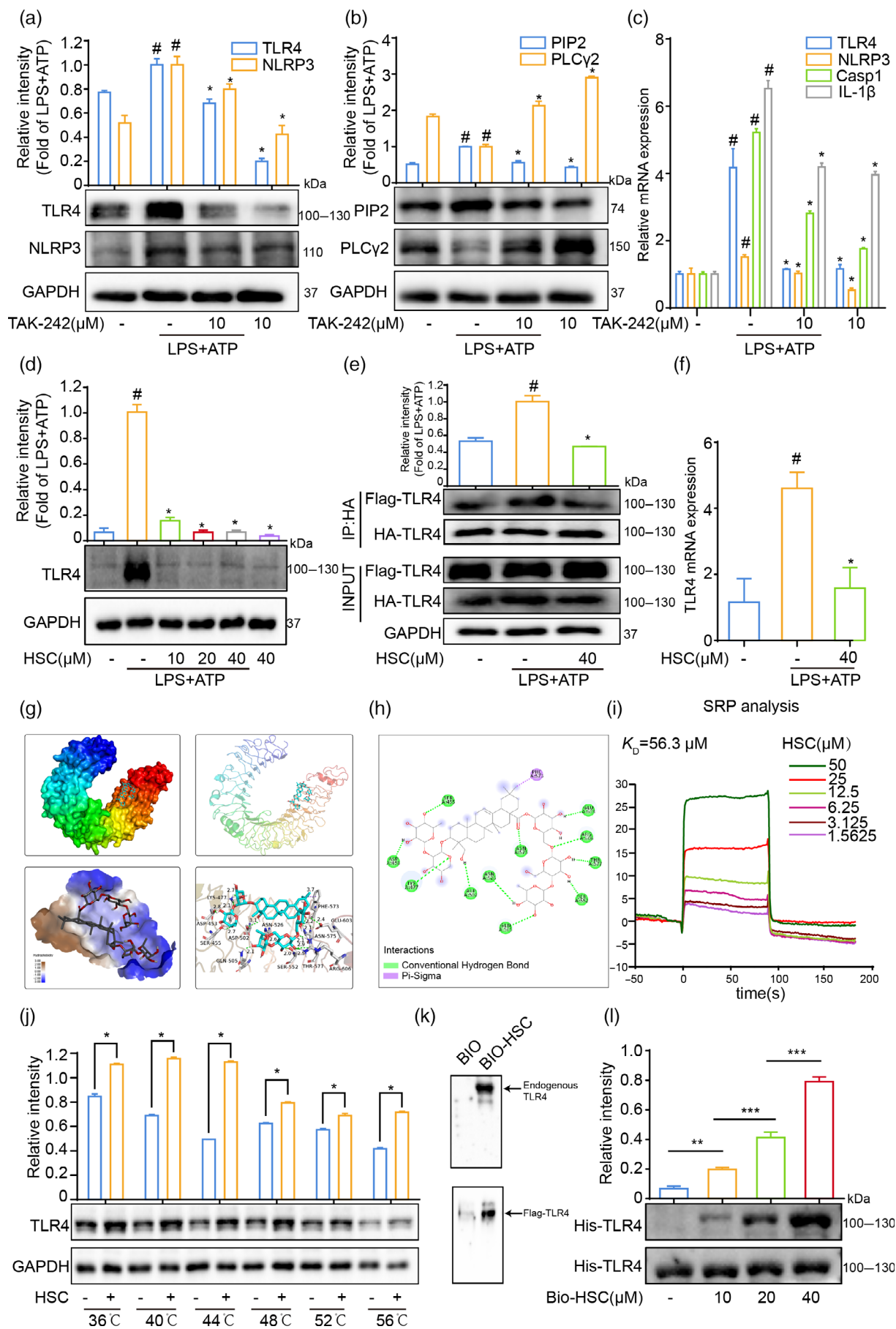


FIGURE 3 HSC inhibited the NF-κB signaling pathway in LPS + ATP-induced HK-2 cells. (a) Phosphorylated and total proteins of TAK1, PKCα, and p65 were identified using western blotting. (b) The results of p-TAK1, p-PKCα, and p-P65 were statistically analyzed. (c–g) The mRNA expression levels of TAK1, PKCα, and p65 were detected using RT-qPCR. (h, i) Western blotting (h) and immunofluorescence (i) were used to confirm the subcellular localization of p65 within the cytoplasm and nucleus of HK-2 cells (Scale bar = 10 μm). #*p* < 0.05, and ###*p* < 0.001 represent significant difference vs. the control group. **p* < 0.05, ***p* < 0.01, and ****p* < 0.001 indicate significant difference vs. the LPS + ATP group. ns, no significance, *n* = 3.



shown in Figure 3a,b, HSC significantly inhibits p-p65, p-TAK1, and p-PKC α in LPS + ATP-stimulated HK-2 cells. HSC was concurrently observed to reduce the mRNA levels of TAK, PKC α , and p65, as illustrated in Figure 3c–e. LPS + ATP triggers the dissociation of NF- κ B/p65 in the cytoplasm, facilitating its translocation to the nucleus in HK-2 cells. However, HSC effectively inhibits this NF- κ B/p65 nuclear translocation, as confirmed by immunofluorescence data (Figure 3h,i). The activation of the NF- κ B signaling pathway leads to the production of pro-inflammatory factors like TNF- α and IL-6 (Li, Yuan, et al., 2021). RT-qPCR, as shown in Figure 3f,g, was used to study the impact of HSC on the release of TNF- α and IL-6. In LPS + ATP-induced HSC cells, TNF- α and IL-6 mRNA expression significantly increased, but HSC was able to reverse this rise. In LPS + ATP-induced HSC cells, TNF- α and IL-6 mRNA expression significantly increased, but HSC was able to curb this rise.

3.4 | HSC targeting TLR4 to suppress the NLRP3 and PIP2 signaling pathways

Studies indicate the regulatory role of TLR4 in NLRP3 inflammasome activation (He et al., 2016). As shown in Figure 4a, the use of TLR4 inhibitor TAK-242 led to a significant decrease in NLRP3 and TLR4 protein expression. RT-qPCR analysis confirmed the decrease of NLRP3, CASP1, and IL-1 β mRNA levels in LPS + ATP-induced HK-2 cells after TAK-242 treatment (Figure 4a,c). TLR4 regulates PIP2 levels by controlling the activities of PIP2 synthetase PIP5K and hydrolase PLC (Kim et al., 2015; Tuosto et al., 2015). As shown in Figure 4b, TAK-242 considerably reduces PIP2 expression and enhances PLC γ 2 expression. The goal was to clarify the influence of TLR4 on NLRP3 activation and the PIP2/PLC γ 2 pathway, in line with previous research (Kim et al., 2015; Wang et al., 2021). As demonstrated in Figure 4d,f, Western blotting and RT-qPCR showed that HSC significantly reduced TLR4 levels in LPS + ATP-stimulated HK-2 cells. This study aimed to investigate the impact of HSC on TLR4 dimerization. Co-transfection of TLR4-HA and TLR4-Flag plasmids into HEK293T cells showed a substantial reduction in TLR4-Flag precipitation due to HSC, suggesting disruption of TLR4 dimerization (Figure 4e).

Molecular docking analysis was employed to determine the specific binding sites of HSC with TLR4. The predicted binding energy of HSC with TLR4 is -37.35 kJ/mol. Analysis indicated that HSC interacts with several residues of TLR4 (Figure 4g,h), a finding further verified by the SPR assay on a Biacore platform. The estimated equilibrium dissociation constant (KD) for the binding of HSC to the TLR4 protein was about 56.3 μ M (Figure 4i). Direct binding of HSC with TLR4 was confirmed by the Cellular Thermal Shift Assay (Figure 4j). We then synthesized a biotin-conjugated HSC probe (HSC-biotin) for the pull-down assay. HSC-biotin precoated streptavidin agarose beads were incubated with 293T-cell lysates, with the precipitated proteins subsequently examined via immunoblotting (IB) to evaluate TLR4 presence. Notably, TLR4 was selectively precipitated by HSC-biotin from both 293T-cell lysates and Flag-TLR4 overexpressed 293T-cell lysates (Figure 4k). Moreover, a concentration-dependent interaction between HSC-biotin and TLR4 was observed (Figure 4l). These results reinforce the proposed interaction between HSC and TLR4.

3.5 | HSC ameliorates LPS-induced AKI in mice

Previous research has identified LPS as a pivotal element in AKI, a condition usually characterized by an abrupt decrease in renal function (Kellum & Prowle, 2018). The study by Han et al. implies a link between elevated WBC counts and an escalated risk of AKI, possibly resulting from neutrophilia and related pro-inflammatory activities (Han et al., 2014). Figure 5a illustrates the administration of LPS to mice, with HSC and DEX treatments given at 0 and 12 h intervals. Hematological findings suggest that HSC treatment effectively mitigates the LPS-induced elevation in WBC, NEU, and Lym in mice suffering from AKI (Figure 5b–d). Creatinine and BUN serve as essential clinical markers for AKI diagnosis (Ronco et al., 2010). LPS treatment notably augmented the levels of creatinine and BUN, a condition significantly alleviated by HSC intervention (Figure 5f,g). Additionally, HE staining revealed that the LPS-induced alterations such as swelling and deformation of renal tubular epithelial cells, edema of renal interstitial epithelial cells, and significant leukocyte infiltration disrupted

FIGURE 4 HSC targeting TLR4 to suppress the NLRP3 and PIP2 signaling pathways. (a,b) HK-2 cells underwent TAK-242 pretreatment for 4 h, followed by a 6 h exposure to LPS, and concluded with ATP incubation at 10 mM for 2 h. Proteins TLR4, NLRP3, PIP2, and PLC γ 2 were detected using western blotting. (c) RT-qPCR was used to identify and quantify messenger RNA levels of TLR4, NLRP3, CASP1, and IL-1 β . (d) Western blotting methodology was again employed to detect TLR4 proteins. (e) HEK293T cells underwent dual transfection with TLR4-HA and TLR4-Flag for 48 h. post-transfection, the cells were treated with 40 μ M of HSC for 4 h, and subsequently stimulated with LPS for 6 h and ATP for 2 h. Co-immunoprecipitation was employed to assess TLR4 dimers. The proteins harvested were then immunoprecipitated with anti-HA magnetic beads, and the immunocomplexes formed were analyzed using western blotting. (f) RT-qPCR was utilized for the quantification of TLR4 mRNA levels. (g, h) Molecular docking analysis was conducted to explore the binding characteristics of HSC to TLR4. (i) Biacore X100 was employed to discern the kinetic and affinity parameters of the HSC-TLR4 interaction. (j) The HSC-TLR4 interaction was examined using the CETSA. (k) Lysates from either 293T cells or those expressing Flag-HSC were incubated with HSC-biotin overnight at 4°C. Subsequently, these lysates underwent streptavidin agarose pull-down assays, and TLR4 was analyzed from the resulting precipitates via Immunoblotting. (l) Recombinant Flag-TLR4 proteins were incubated with HSC-biotin for 1 h at 37°C, followed by an Immunoblotting using biotin (upper band) or His (lower band). # p < 0.05 represents significant difference vs. the control group. * p < 0.05, ** p < 0.01, and *** p < 0.001 indicate significant difference vs. the LPS + ATP or control group, n = 3.

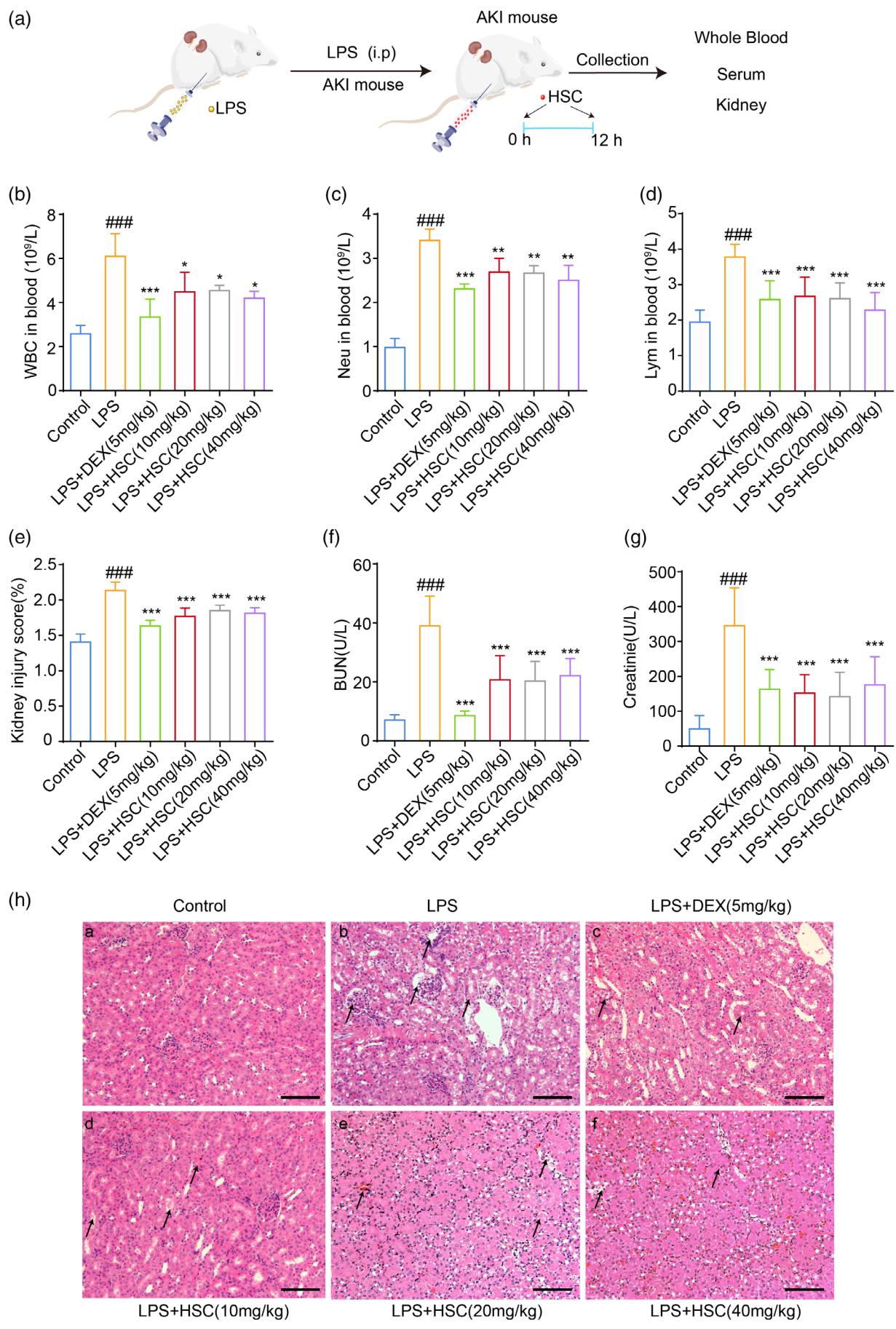


FIGURE 5 Legend on next page.

the standard structure of renal tissues. When compared to the LPS model group, pre-treatment with HSC significantly mitigated the severity of LPS-induced AKI (Figure 5h), with DEX serving as the positive control group. In summary, HSC treatment significantly mitigates the onset of LPS-induced AKI.

3.6 | HSC inhibits the production of inflammatory factors by regulating the NF- κ B, NLRP3, and PIP2 pathways

Studies have demonstrated a close association between the levels of TNF- α and IL-6 and renal tubular injury (Patel et al., 2005; Ramesh & Reeves, 2002). IL-1 β is instrumental in the development and progression of renal tissue inflammation and injury (Faggioni et al., 1998). ELISA analysis revealed a significant downregulation of LPS-induced TNF- α (Figure 6a), IL-6 (Figure 6b), and IL-1 β (Figure 6c) in the serum of HSC-treated mice compared to LPS mice. Likewise, HSC significantly suppressed the LPS-induced up-regulation of TNF- α , IL-6, IL-1 β in renal tissue (Figure 6d–f). Our research indicates that HSC mitigates LPS-induced renal inflammation, yielding effects analogous to the positive control drug, DEX. Recent investigations have suggested that the renal NF- κ B pathway is implicated in the pathogenesis of LPS-induced AKI (Zhang et al., 2018). We analyzed the impact of HSC pre-treatment on the activation of the renal NF- κ B signaling pathway induced by LPS. As anticipated, the expression of phosphorylated TLR4, TAK1, PKC α , and p65 proteins was significantly elevated in the renal tissue of LPS-induced AKI mice, while HSC markedly attenuated this expression (Figure 6g). Prior studies have established that the activation of the NLRP3 inflammasome and IL-1 β is integral to the pathogenesis of LPS-induced AKI and exacerbation of renal functional injury (Lin et al., 2019). Western blotting analysis suggested significant upregulation of NLRP3, cleaved caspase-1, and cleaved IL-1 β in the LPS group, whereas a pronounced repression was observed in the HSC and DEX groups (Figure 6h). DAG and IP3, significant second messengers, respectively, govern PKC activity and the release of intracellular calcium from the endoplasmic reticulum (Exton, 2000). They further modulate the inflammatory response by influencing the activation of NF- κ B and NLRP3 inflammasome response by modulating the activation of NF- κ B and NLRP3 inflammasome (Moscat et al., 2003; Murakami et al., 2012). Figure 6i demonstrates that HSC fosters the degradation of LPS-induced PLC γ 2 protein. Moreover, HSC treatment could reverse the LPS-induced increase in PIP2, DAG, and IP3. These findings indicate that HSC mitigates AKI in mice by modulating the NF- κ B, NLRP3, and PIP2 pathways.

4 | DISCUSSION

Traditional Chinese Medicine (TCM) treats kidney injury by reducing oxidative stress and exhibiting anti-inflammatory effects (Han et al., 2022). The study found that hesperidin, a natural antioxidant, has a protective effect against kidney injury caused by dust storm particulate matter in rats (Sarkaki et al., 2023). Additionally, Gallic acid demonstrated protective properties against cisplatin-induced nephrotoxicity in rats by reducing oxidative stress, inflammation, and apoptosis, and enhancing the expression of the long non-coding RNA TUG1 (Amini et al., 2022). Preliminary research found HSC exhibits potent anti-inflammatory effects by targeting the PIP2/NF- κ B/NLRP3 signaling pathway, offering potential as a therapeutic agent for treating acute lung injury (ALI) (Han et al., 2022). HSC shows potential for treating ulcerative colitis through its anti-inflammatory effects, as evidenced by pharmacokinetics-pharmacodynamics modeling and cytokine level changes in colitis rats (Zhou et al., 2022). In addition, HSC displayed potent antioxidant activity, with HSC at 75 μ g/mL demonstrating 86% inhibition of lipid peroxidation in linoleic acid emulsion (Gülçin et al., 2004).

In this study, the LPS-induced AKI model and LPS + ATP-induced HK2 cells were employed to explore the anti-inflammatory mechanisms of HSC in AKI. In this study, we investigated the effects of HSC on LPS-induced AKI and explored the underlying mechanisms involved. Our results demonstrated that LPS administration led to AKI, as evidenced by increased serum creatinine and blood urea nitrogen (BUN) levels and histological changes in the kidney. However, HSC treatment effectively ameliorated the kidney dysfunction induced by LPS. Furthermore, we observed that HSC exerted its protective effects by targeting the TLR4-regulated NF- κ B and PIP2 signaling pathways, leading to the suppression of NLRP3 inflammasome activation. These findings suggest that HSC holds promise as a potential therapeutic agent for AKI by modulating inflammatory responses and cellular signaling pathways.

Sepsis, a complex disease, is characterized by an irregular response to an active infection caused by invading microorganisms or their byproducts (Stasi et al., 2017). AKI, a disease often linked to sepsis, emerges as a significant complication characterized by impaired kidney function and a high fatality rate, often induced by LPS (Anders et al., 2004; Chu et al., 2016). The pathogenesis of AKI is primarily highlighted by kidney tubular inflammation, which often coincides with kidney injury (Eftekhari et al., 2020; Ye et al., 2017). This tubular inflammation, triggered by LPS-induced AKI, activates vacuoles in kidney cells, signifying a moderate to severe level of renal injury (Tang et al., 2018). This process also stimulates an

FIGURE 5 HSC ameliorates LPS-induced AKI in mice. (a) The mice were administrated with LPS (2 mg/kg, i.p.), then treated by HSC (10, 20, and 40 mg/kg, i.p.), and DEX (5 mg/kg, i.p.) at 0, 12 h. The mice were sacrificed, and the whole blood, kidney, and serum were collected. (b) The counts of white blood cells (WBC). (c) The counts of neutrophils (NEU). (d) The counts of Lymphocytes (Lym). (e) Kidney index; (f) blood urea nitrogen (BUN); (g) creatinine was evaluated after LPS induction for 24 h. (h) Kidney histopathology was assessed via HE stains assay at 24 h after LPS challenge (200 \times). Arrows indicated the lesion or swelling or necrosis or inflammatory infiltration of the kidney tissues. ### $p < 0.01$ represents significant difference vs. the control group. * $p < 0.05$ and *** $p < 0.001$ indicate significant difference vs. the LPS group, $n = 6$.

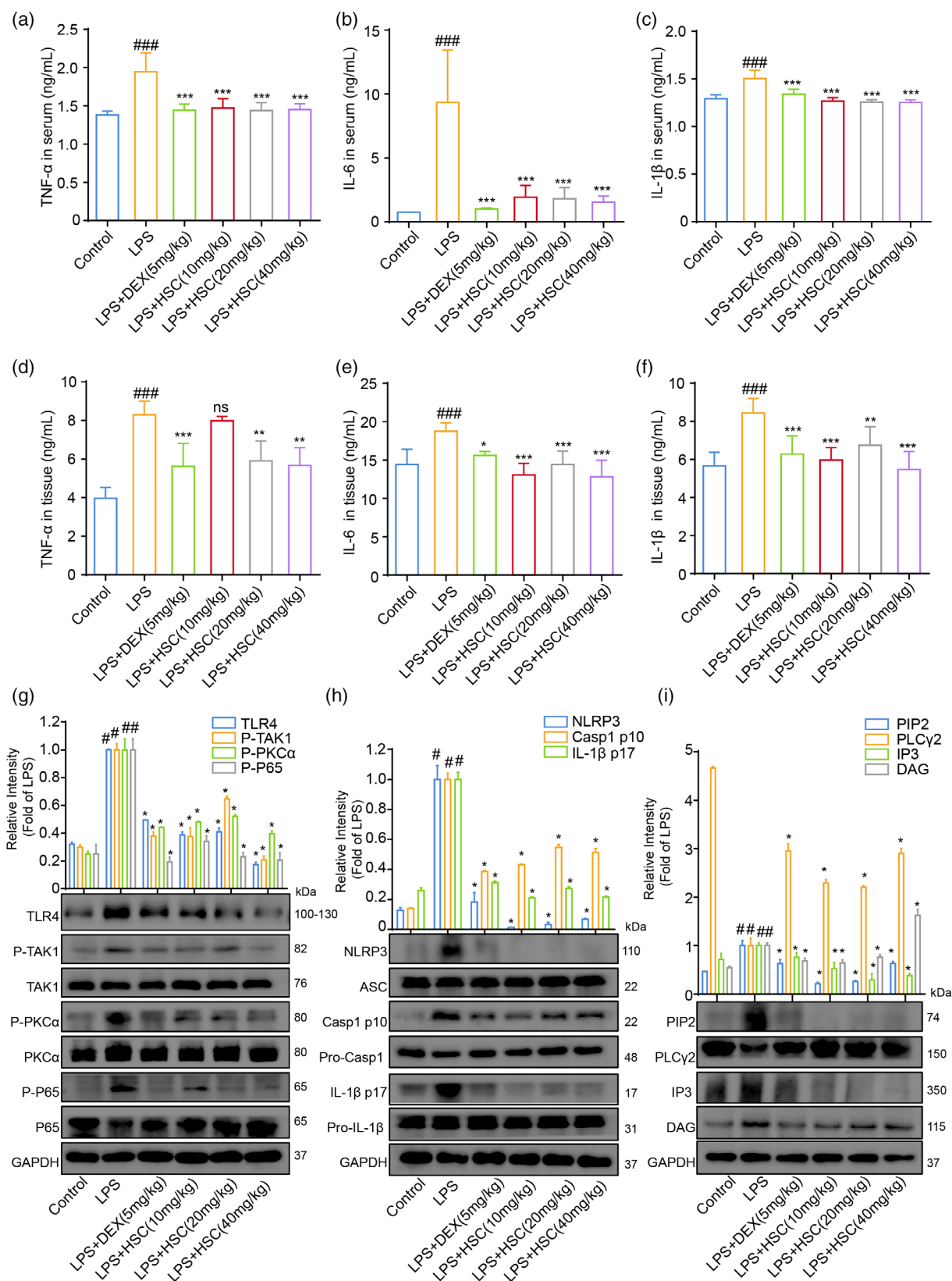


FIGURE 6 HSC inhibits the production of inflammatory factors by regulating the NF-κB, NLRP3, and PIP2 pathways. (a–f) The release of TNF-α, IL-6, and IL-1β in serum (a–c) and kidney tissue (d–f) were detected by ELISA kits. (g) The proteins TLR4, TAK1, PKCα, and p65 were detected by western blotting. (h) NLRP3 inflammasome-related proteins NLRP3, ASC, casp1 p10, pro-casp1, IL-1β p17, and pro-IL-1β were detected by western blotting. (i) PIP2 signaling pathways related proteins to PIP2, PLCγ2, IP3, and DAG were detected by western blotting. #*p* < 0.05, ###*p* < 0.001 represent significant difference vs. the control group. **p* < 0.05, ***p* < 0.01, ****p* < 0.001 indicate significant difference vs. the LPS group. ns, no significance, *n* = 6.

increase in the secretion of creatinine and BUN (Alsharif et al., 2020). Our study has found that treatment with HSC significantly alleviates this kidney dysfunction by reducing the levels of serum creatinine and BUN. Moreover, it substantially mitigates kidney tubular injury following LPS induction, highlighting the potent role of HSC in combating septic AKI.

AKI, often triggered by LPS, presents a significant clinical challenge due to its abrupt onset and severe consequences. Extensive research indicates that TLR4 plays a pivotal role in modulating LPS-induced AKI as the primary LPS sensor and as an integral part of subsequent inflammatory responses (Hu et al., 2022). TLR4 has been found to regulate the activation of downstream inflammatory cascades, thereby exacerbating kidney injury (Cui et al., 2021). In our study, we found that HSC selectively binds to and inhibits TLR4 activity. This inhibition subsequently curtails the activation of the NF- κ B pathway and diminishes the production of pro-inflammatory cytokines, such as TNF- α , IL-6, and IL-1 β . Our results suggested that HSC downregulates the expression p-TAK1, p-PKC α , and p-p65, which further inhibits NF- κ B activation in LPS + ATP-induced HK-2 cells and LPS-induced AKI mice. Moreover, TLR4 has been linked with the activation of the NLRP3 inflammasome, a cytosolic complex involved in the maturation and secretion of inflammatory cytokines (Corpetti et al., 2021). This inflammasome, upon activation, overexpresses cleaved caspase-1 and mature IL-1 β , resulting in NEU recruitment and the consequent progression of AKI (Danielski et al., 2020). Our results suggested that HSC decreased the expression NLRP3, CASP1, and IL-1 β , which further inhibits LPS + ATP-induced NLRP3 inflammasome activity. Specifically, during an AKI episode, LPS-activated TLR4 instigates the assembly of the NLRP3 inflammasome, thereby driving a potent inflammatory response and cellular death, both of which intensify renal injury. In this research, we applied the TLR4 inhibitor TAK-242 and observed a significant decline in NLRP3 protein expression. TAK-242 also decreased the mRNA levels of NLRP3, CASP1, and IL-1 β , which are instrumental in inhibiting the NLRP3 inflammasome activity.

The PIP2 signaling pathway stands as another crucial mechanism regulated by TLR4 within the context of AKI. PIP2 serves as a precursor for secondary messengers like DAG and IP3, which are instrumental in intracellular signaling pertaining to inflammation and cell survival (Li et al., 2023). Our results showed that HSC decreased the expression of PIP2, DAG, and IP3 and increased the expression of PLC γ 2 in LPS + ATP-induced HK-2 cells and LPS-induced AKI mice. HSC may reduce the expression of PIP2, which affects the hydrolysis of PLC γ 2 substrates, resulting in an increase in the expression of PLC γ 2. Therefore, HSC reduces intracellular Ca²⁺ levels by the PIP2 signaling pathway. In addition, HSC inhibited the serum and kidney production of pro-inflammatory cytokines TNF- α , IL-6, and IL-1 β in LPS-stimulated AKI. TLR4 is proven to govern the PIP2 pathway, influencing the release of intracellular calcium and contributing to the AKI-associated inflammatory response (Gupta et al., 2020). We observed that TAK-242 could inhibit PIP2 and PLC γ 2 protein expression. Furthermore, the PIP2 signaling pathway is intimately linked with the activation of the NLRP3 inflammasome (Wani

et al., 2021). Our study demonstrated that HSC exerts an anti-inflammatory effect by suppressing the NF- κ B signaling pathway. Additionally, HSC inhibited the activation of the PIP2 signaling pathway, which subsequently stifled the activation of the NLRP3 inflammasome.

Our research findings demonstrate that HSC exerts its inhibitory effects on NLRP3 inflammasome activation by targeting the TLR4-regulated NF- κ B and PIP2 signaling pathways. This uncovers previously unrecognized anti-inflammatory mechanisms of HSC, indicating that its therapeutic approach of TLR4 modulation for AKI differs from current clinical methods such as dialysis and antibiotic treatments. HSC has the potential to serve as a viable alternative or supplementary treatment strategy. While we have elucidated the potential anti-inflammatory mechanisms of HSC, there is a possibility that we might have overlooked other complex pathways contributing to AKI or broader inflammatory responses, such as diabetic nephropathy (Eftekhari et al., 2020). Furthermore, our study's scope was confined to a specific model of AKI induced by LPS, leaving the effectiveness of HSC against alternative causes of AKI yet to be explored. HSC has antioxidant effect and has the potential to be applied in the field of nano-biotechnology. For example, the extract of *Scutellaria baicalensis* plays an important role in the formation and stabilization of silver nanoparticles (Ahmadov et al., 2020).

AUTHOR CONTRIBUTIONS

Shan Han: Validation; writing – original draft. **Siyuan Li:** Validation. **Jilang Li:** Validation. **Jia He:** Data curation; formal analysis. **Qin-Qin Wang:** Data curation; formal analysis. **Xiang Gao:** Data curation; formal analysis. **Shilin Yang:** Writing – review and editing. **Jingjing Li:** Writing – original draft. **Renyikun Yuan:** Conceptualization; writing – original draft. **Guoyue Zhong:** Writing – review and editing. **Hongwei Gao:** Conceptualization; writing – review and editing.

ACKNOWLEDGMENTS

Authors gratefully acknowledge the financial support.

FUNDING INFORMATION

We would like to appreciate the support from the project of Guangxi Science and Technology Base and Talent Project (2022AC18022), the China-ASEAN International Innovative Center for Health Industry of TCM (AD20297142), Qihuang High-level Talent Team Cultivation Project of Guangxi University of Chinese Medicine (2021002), Guangxi overseas “100 persons' plan” high-level expert, the Innovation Project of Guangxi Graduate Education (YCSW2019176), University of Chinese Medicine (2022BS008), Guangxi University Young and Middle-Aged Teachers Research Basic Ability Improvement Project (2023KY0303), and Jiangxi Province 2022 Annual Graduate Student Innovation Special Fund Project (YC2022-B189).

CONFLICT OF INTEREST STATEMENT

The authors declare that they have no competing interests.

DATA AVAILABILITY STATEMENT

The data that support the findings of this study are available from the corresponding author upon reasonable request. The source data for original uncropped blot/gel images have been uploaded as part of the Supporting Inform.

CONSENT FOR PUBLICATION

We declare that the Publisher has the Author's permission to publish the relevant contribution.

ORCID

Jingjing Li  <https://orcid.org/0000-0003-3636-0537>

Renyikun Yuan  <https://orcid.org/0000-0001-8590-4364>

Hongwei Gao  <https://orcid.org/0000-0001-9179-750X>

REFERENCES

- Ahmadvov, I., Bandalayeva, A., Nasibova, A., Hasanova, F., & Khalilov, R. (2020). The synthesis of the SILVER nanodrugs IN the medicinal plant BAIKAL skullcap (SCUTELLARIA BAICALENSIS GEORGI) and their antioxidant, antibacterial activity. *Advances in Biology & Earth Sciences*, 5(2), 103–118.
- Alsharif, K. F., Almalki, A. A., Al-Amer, O., Mufti, A. H., Theyab, A., Lokman, M. S., Ramadan, S. S., Almeer, R. S., Hafez, M. M., Kassab, R. B., & Abdel Moneim, A. E. (2020). Oleuropein protects against lipopolysaccharide-induced sepsis and alleviates inflammatory responses in mice. *IUBMB Life*, 72(10), 2121–2132. <https://doi.org/10.1002/iub.2347>
- Amini, N., Badavi, M., Mard, S. A., Dianat, M., & Moghadam, M. T. (2022). The renoprotective effects of gallic acid on cisplatin-induced nephrotoxicity through anti-apoptosis, anti-inflammatory effects, and down-regulation of lncRNA TUG1. *Naunyn-Schmiedeberg's Archives of Pharmacology*, 395(6), 691–701. <https://doi.org/10.1007/s00210-022-02227-1>
- Anders, H. J., Banas, B., & Schlöndorff, D. (2004). Signaling danger: Toll-like receptors and their potential roles in kidney disease. *Journal of the American Society of Nephrology*, 15(4), 854–867. <https://doi.org/10.1097/01.asn.0000121781.89599.16>
- Banerjee, R., Samanta, M., & Das, S. (2020). NF- κ B signaling induces inductive expression of the downstream molecules and IgD gene in the freshwater carp, *Catla catla*. 3 *Biotech*, 10(10), 445–1065. <https://doi.org/10.1038/sj.bjp.0704334>
- Chu, X.-Q., Wang, L., Li, W., Duya, P., & Bian, Y.-H. (2016). Effect of Chinese materia medica with tonifying kidney function on transplantation of multipotency mesenchymal stem cells from human umbilical cord in mice model of acute kidney injury. *Chinese Herbal Medicines*, 8(2), 173–181. [https://doi.org/10.1016/S1674-6384\(16\)60027-8](https://doi.org/10.1016/S1674-6384(16)60027-8)
- Corpetti, C., Del Re, A., Seguela, L., Palencia, I., Rurgo, S., De Conno, B., Pesce, M., Sarneli, G., & Esposito, G. (2021). Cannabidiol inhibits SARS-Cov-2 spike (S) protein-induced cytotoxicity and inflammation through a PPAR γ -dependent TLR4/NLRP3/Caspase-1 signaling suppression in Caco-2 cell line. *Phytotherapy Research*, 35(12), 6893–6903. <https://doi.org/10.1002/ptr.7302>
- Cui, Y., Gao, H., Han, S., Yuan, R., He, J., Zhuo, Y., Feng, Y. L., Tang, M., Feng, J., & Yang, S. (2021). Oleuropein attenuates lipopolysaccharide-induced acute kidney injury in vitro and in vivo by regulating toll-like receptor 4 dimerization. *Frontiers in Pharmacology*, 12, 617314. <https://doi.org/10.3389/fphar.2021.617314>
- Danielski, L. G., Giustina, A. D., Bonfante, S., Barichello, T., & Petronilho, F. (2020). The NLRP3 inflammasome and its role in sepsis development. *Inflammation*, 43(1), 24–31. <https://doi.org/10.1007/s10753-019-01124-9>
- Eftekhari, A., Vahed, S. Z., Kavetsky, T., Rameshrad, M., Jafari, S., Chodari, L., Hosseiniyan, S. M., Derakhshankhah, H., Ahmadian, E., & Ardalan, M. (2020). Cell junction proteins: Crossing the glomerular filtration barrier in diabetic nephropathy. *International Journal of Biological Macromolecules*, 148, 475–482. <https://doi.org/10.1016/j.ijbiomac.2020.01.168>
- Exton, J. H. (2000). Phospholipases. In P. M. Conn & A. R. Means (Eds.), *Principles of molecular regulation*. Humana Press. https://doi.org/10.1007/978-1-59259-032-2_13
- Faggioni, R., Fantuzzi, G., Fuller, J., Dinarello, C. A., Feingold, K. R., & Grunfeld, C. (1998). IL-1 beta mediates leptin induction during inflammation. *The American Journal of Physiology*, 274(1), R204–R208. <https://doi.org/10.1152/ajpregu.1998.274.1.R204>
- Gepdiremen, A., Mshvildadze, V., Süleyman, H., & Elias, R. (2005). Acute anti-inflammatory activity of four saponins isolated from ivy: Alpha-hederin, hederasaponin-C, hederacolchiside-E and hederacolchiside-F in carrageenan-induced rat paw edema. *Phytomedicine*, 12(6–7), 440–444. <https://doi.org/10.1016/j.phymed.2004.04.005>
- Gülçin, I., Mshvildadze, V., Gepdiremen, A., & Elias, R. (2004). Antioxidant activity of saponins isolated from ivy: Alpha-hederin, hederasaponin-C, hederacolchiside-E and hederacolchiside-F. *Planta Medica*, 70(6), 561–563. <https://doi.org/10.1055/s-2004-827158>
- Gupta, A., Kumar, D., Puri, S., & Puri, V. (2020). Neuroimmune mechanisms in signaling of pain during acute kidney injury (AKI). *Frontiers in Medicine*, 7, 424. <https://doi.org/10.3389/fmed.2020.00424>
- Han, S., Gao, H., Chen, S., Wang, Q., Li, X., Du, L.-J., Li, J., Luo, Y. Y., Li, J. X., Zhao, L. C., Feng, J., & Zhao, L.-C. (2019). Procyanidin A1 alleviates inflammatory response induced by LPS through NF- κ B, MAPK, and Nrf2/HO-1 pathways in RAW264. 7 cells. *Scientific Reports*, 9(1), 15087. <https://doi.org/10.1038/s41598-019-51614-x>
- Han, S., Yuan, R., Cui, Y., He, J., Wang, Q. Q., Zhuo, Y., Yang, S., & Gao, H. (2022). Hederasaponin C alleviates lipopolysaccharide-induced acute lung injury In vivo and In vitro through the PIP2/NF- κ B/NLRP3 signaling pathway. *Frontiers in Immunology*, 13, 846384. <https://doi.org/10.3389/fimmu.2022.846384>
- Han, S. S., Ahn, S. Y., Ryu, J., Baek, S. H., Kim, K. I., Chin, H. J., Na, K. Y., Chae, D.-W., & Kim, S. (2014). U-shape relationship of white blood cells with acute kidney injury and mortality in critically ill patients. *The Tohoku Journal of Experimental Medicine*, 232(3), 177–185. <https://doi.org/10.1620/tjem.232.177>
- He, J., Yuan, R., Cui, X., Cui, Y., Han, S., Wang, Q. Q., Chen, Y., Huang, L., Yang, S., Xu, Q., Zhao, Y., & Gao, H. (2020). Anemoside B4 protects against Klebsiella pneumoniae- and influenza virus FM1-induced pneumonia via the TLR4/MyD88 signaling pathway in mice. *Chinese Medicine*, 15, 68. <https://doi.org/10.1186/s13020-020-00350-w>
- He, Y., Hara, H., & Núñez, G. (2016). Mechanism and regulation of NLRP3 inflammasome activation. *Trends in Biochemical Sciences*, 41(12), 1012–1021. <https://doi.org/10.1016/j.tibs.2016.09.002>
- Hu, X., Zhou, W., Wu, S., Wang, R., Luan, Z., Geng, X., Xu, N., Zhang, Z., Ruan, Z., Wang, Z., Li, F., Yu, C., & Ren, H. (2022). Tacrolimus alleviates LPS-induced AKI by inhibiting TLR4/MyD88/NF- κ B signalling in mice. *Journal of Cellular and Molecular Medicine*, 26(2), 507–514. <https://doi.org/10.1111/jcmm.17108>
- Jin, M. M., Zhang, W. D., Song, G. S., Xu, Y. M., Du, Y. F., Guo, W., Cao, L., & Xu, H. J. (2018). Discrimination and chemical phylogenetic study of four Pulsatilla herbs using UPLC-ESI-MS/MS combined with hierarchical cluster analysis. *Journal of Chromatographic Science*, 56(3), 216–224. <https://doi.org/10.1093/chromsci/bmx102>
- Kellum, J. A., & Prowle, J. R. (2018). Paradigms of acute kidney injury in the intensive care setting. *Nature Reviews Nephrology*, 14(4), 217–230. <https://doi.org/10.1038/nrneph.2017.184>
- Kim, K. S., Jang, J. H., Lin, H., Choi, S. W., Kim, H. R., Shin, D. H., Nam, J. H., Zhang, Y. H., & Kim, S. J. (2015). Rise and fall of Kir2. 2 current by TLR4 signaling in human monocytes: PKC-dependent

- trafficking and PI3K-mediated PIP2 decrease. *The Journal of Immunology*, 195(7), 3345–3354. <https://doi.org/10.4049/jimmunol.1500056>
- Li, S., Yuan, R., Fan, Q., Zhang, C., Han, S., Li, J., Xu, Z., Sun, K., Xu, Q., Yao, C., & Yang, S. (2023). Ginsenoside Rb1 exerts therapeutic effects on ulcerative colitis through regulating the Nrf2/PIP2/NLRP3 inflammasome signaling pathway. *Journal of Functional Foods*, 102, 105475. <https://doi.org/10.1016/j.jff.2023.105475>
- Li, X., Zou, Y., Fu, Y.-Y., Xing, J., Wang, K.-Y., Wan, P.-Z., Wang, M., & Zhai, X.-Y. (2021). Ibudilast attenuates folic acid-induced acute kidney injury by blocking pyroptosis through TLR4-mediated NF- κ B and MAPK signaling pathways. *Frontiers in Pharmacology*, 12, 650283. <https://doi.org/10.3389/fphar.2021.650283>
- Li, X. X., Yuan, R., Wang, Q. Q., Han, S., Liu, Z., Xu, Q., Yang, S., & Gao, H. (2021). Rotundic acid reduces LPS-induced acute lung injury in vitro and in vivo through regulating TLR4 dimer. *Phytotherapy Research*, 35(8), 4485–4498. <https://doi.org/10.1002/ptr.7152>
- Lin, Q., Li, S., Jiang, N., Shao, X., Zhang, M., Jin, H., Zhang, Z., Shen, J., Zhou, Y., Zhou, W., Gu, L., Lu, R., & Ni, Z. (2019). PINK1-parkin pathway of mitophagy protects against contrast-induced acute kidney injury via decreasing mitochondrial ROS and NLRP3 inflammasome activation. *Redox Biology*, 26, 101254. <https://doi.org/10.1016/j.redox.2019.101254>
- Liu, N., Gao, Y., Liu, Y., & Liu, D. (2023). GBP5 inhibition ameliorates the progression of lupus nephritis by suppressing NLRP3 inflammasome activation. *Immunological Investigations*, 52(1), 52–66. <https://doi.org/10.1080/08820139.2022.2122834>
- Lozano, J., Berra, E., Municio, M. M., Diaz-Meco, M. T., Dominguez, I., Sanz, L., & Moscat, J. (1994). Protein kinase C zeta isoform is critical for kappa B-dependent promoter activation by sphingomyelinase. *The Journal of Biological Chemistry*, 269(30), 19200–19202.
- Moscat, J., Diaz-Meco, M. T., & Rennert, P. (2003). NF- κ B activation by protein kinase C isoforms and B-cell function. *EMBO Reports*, 4(1), 31–36. <https://doi.org/10.1038/sj.embor.embor704>
- Murakami, T., Ockinger, J., Yu, J., Byles, V., McColl, A., Hofer, A. M., & Horng, T. (2012). Critical role for calcium mobilization in activation of the NLRP3 inflammasome. *Proceedings of the National Academy of Sciences*, 109(28), 11282–11287. <https://doi.org/10.1073/pnas.1117765109>
- Oweis, A. O., Alshelleh, S. A., Momany, S. M., Samrah, S. M., Khassawneh, B. Y., & Al Ali, M. A. K. (2020). Incidence, risk factors, and outcome of acute kidney injury in the intensive care unit: A single-center study from Jordan. *Critical Care Research and Practice*, 2020, 8753764. <https://doi.org/10.1155/2020/8753764>
- Patel, N. S., Chatterjee, P. K., Di Paola, R., Mazzon, E., Britti, D., De Sarro, A., Cuzzocrea, S., & Thiemermann, C. (2005). Endogenous interleukin-6 enhances the renal injury, dysfunction, and inflammation caused by ischemia/reperfusion. *The Journal of Pharmacology and Experimental Therapeutics*, 312(3), 1170–1178. <https://doi.org/10.1124/jpet.104.078659>
- Pham, T. H., Kim, M. S., Le, M. Q., Song, Y. S., Bak, Y., Ryu, H. W., Oh, S.-R., & Yoon, D. Y. (2017). Fargesin exerts anti-inflammatory effects in THP-1 monocytes by suppressing PKC-dependent AP-1 and NF- κ B signaling. *Phytomedicine*, 24, 96–103. <https://doi.org/10.1016/j.phymed.2016.11.014>
- Ramesh, G., & Reeves, W. B. (2002). TNF- α mediates chemokine and cytokine expression and renal injury in cisplatin nephrotoxicity. *The Journal of Clinical Investigation*, 110(6), 835–842. <https://doi.org/10.1172/jci15606>
- Ronco, C., Grammaticopoulos, S., Rosner, M., De Cal, M., Soni, S., Lentini, P., & Piccinni, P. (2010). Oliguria, creatinine and other biomarkers of acute kidney injury. *Contributions to Nephrology*, 164, 118–127. <https://doi.org/10.1159/000313725>
- Sarkaki, A., Badavi, M., Nejaddehbash, F., Hajipour, S., Basir, Z., & Amini, N. (2023). The renoprotective effects of hesperidin on kidney injury induced by exposure to severe chronic dust storm particulate matter through inhibiting the Smads/TGF- β 1 signaling in rat. *Naunyn-Schmiedeberg's Archives of Pharmacology*, 396(4), 1–12. <https://doi.org/10.1007/s00210-023-02562-x>
- Stasi, A., Intini, A., Divella, C., Franzin, R., Montemurno, E., Grandaliano, G., Ronco, C., Fiaccadori, E., Pertosa, G. B., Gesualdo, L., & Castellano, G. (2017). Emerging role of lipopolysaccharide binding protein in sepsis-induced acute kidney injury. *Nephrology Dialysis Transplantation*, 32(1), 24–31. <https://doi.org/10.1093/ndt/gfw250>
- Suh, P. G., Park, J. I., Manzoli, L., Cocco, L., Peak, J. C., Katan, M., Fukami, K., Kataoka, T., Yun, S., & Ryu, S. H. (2008). Multiple roles of phosphoinositide-specific phospholipase C isozymes. *BMB Reports*, 41(6), 415–434. <https://doi.org/10.5483/bmbrep.2008.41.6.415>
- Tang, Y., Wang, C., Wang, Y., Zhang, J., Wang, F., Li, L., Meng, X., Li, G., Li, Y., & Wang, L. (2018). Isoliquiritigenin attenuates LPS-induced AKI by suppression of inflammation involving NF- κ B pathway. *American Journal of Translational Research*, 10(12), 4141–4151.
- Tuosto, L., Capuano, C., Muscolini, M., Santoni, A., & Galandini, R. (2015). The multifaceted role of PIP2 in leukocyte biology. *Cellular and Molecular Life Sciences*, 72, 4461–4474. <https://doi.org/10.1007/s00018-015-2013-0>
- Vallés, P. G., Gil Lorenzo, A. F., Garcia, R. D., Cacciamani, V., Benardon, M. E., & Costantino, V. V. (2023). Toll-like receptor 4 in acute kidney injury. *International Journal of Molecular Sciences*, 24(2), 1415. <https://doi.org/10.3390/ijms24021415>
- Vázquez-Carballo, C., Guerrero-Hue, M., García-Caballero, C., Rayego-Mateos, S., Opazo-Ríos, L., Morgado-Pascual, J. L., Herencia-Bellido, C., Vallejo-Mudarra, M., Cortegano, I., Gaspar, M. L., de Andrés, B., Egido, J., & Moreno, J. A. (2021). Toll-like receptors in acute kidney injury. *International Journal of Molecular Sciences*, 22(2), 816. <https://doi.org/10.3390/ijms22020816>
- Wang, H., Huang, M., Wang, W., Zhang, Y., Ma, X., Luo, L., Xu, X., Xu, L., Shi, H., Xu, Y., Wang, A., & Xu, Y. (2021). Microglial TLR4-induced TAK1 phosphorylation and NLRP3 activation mediates neuroinflammation and contributes to chronic morphine-induced antinociceptive tolerance. *Pharmacological Research*, 165, 105482. <https://doi.org/10.1016/j.phrs.2021.105482>
- Wang, L., Negro, R., & Wu, H. (2020). TRPM2, linking oxidative stress and Ca²⁺ permeation to NLRP3 inflammasome activation. *Current Opinion in Immunology*, 62, 131–135. <https://doi.org/10.1016/j.coi.2020.01.005>
- Wani, K., AlHarthi, H., Alghamdi, A., Sabico, S., & Al-Daghri, N. M. (2021). Role of NLRP3 inflammasome activation in obesity-mediated metabolic disorders. *International Journal of Environmental Research and Public Health*, 18(2), 511. <https://doi.org/10.3390/ijerph18020511>
- Wu, J., Powell, F., Larsen, N. A., Lai, Z., Byth, K. F., Read, J., Gu, R. F., Roth, M., Toader, D., Saeh, J. C., & Chen, H. (2013). Mechanism and in vitro pharmacology of TAK1 inhibition by (5Z)-7-Oxozeaenol. *ACS Chemical Biology*, 8(3), 643–650. <https://doi.org/10.1021/cb3005897>
- Wu, X., Gao, H., Sun, W., Yu, J., Hu, H., Xu, Q., & Chen, X. (2017). Nepetoidin B, a natural product, inhibits LPS-stimulated nitric oxide production via modulation of iNOS mediated by NF- κ B/MKP-5 pathways. *Phytotherapy Research*, 31(7), 1072–1077. <https://doi.org/10.1002/ptr.5828>
- Ye, H. Y., Jin, J., Jin, L. W., Chen, Y., Zhou, Z. H., & Li, Z. Y. (2017). Chlorogenic acid attenuates lipopolysaccharide-induced acute kidney injury by inhibiting TLR4/NF- κ B signal pathway. *Inflammation*, 40(2), 523–529. <https://doi.org/10.1007/s10753-016-0498-9>
- Yuan, R., Li, Y., Han, S., Chen, X., Chen, J., He, J., Gao, H., Yang, Y., Yang, S., & Yang, Y. (2022). Fe-curcumin nanozyme-mediated reactive

oxygen species scavenging and anti-inflammation for acute lung injury. *ACS Central Science*, 8(1), 10–21. <https://doi.org/10.1021/acscentsci.1c00866>

Zhang, F., Lu, S., Jin, S., Chen, K., Li, J., Huang, B., & Cao, Y. (2018). Lidan-paidu prescription alleviates lipopolysaccharide-induced acute kidney injury by suppressing the NF- κ B signaling pathway. *Biomedicine & Pharmacotherapy*, 99, 245–252. <https://doi.org/10.1016/j.biopha.2018.01.059>

Zhou, B. C., Tian, Y. G., Sun, Y. N., Liu, Y. L., & Zhao, D. (2022). A validated LC-MS/MS method for the determination of hederasaponin C: Application to pharmacokinetics-pharmacodynamics studies in the therapeutic area of acetic acid-induced ulcerative colitis in rats. *Bio-medical Chromatography*, 36(10), e5450. <https://doi.org/10.1002/bmc.5450>

SUPPORTING INFORMATION

Additional supporting information can be found online in the Supporting Information section at the end of this article.

How to cite this article: Han, S., Li, S., Li, J., He, J., Wang, Q.-Q., Gao, X., Yang, S., Li, J., Yuan, R., Zhong, G., & Gao, H. (2023). Hederasaponin C inhibits LPS-induced acute kidney injury in mice by targeting TLR4 and regulating the PIP2/NF- κ B/NLRP3 signaling pathway. *Phytotherapy Research*, 37(12), 5974–5990. <https://doi.org/10.1002/ptr.8014>